

# CNN as Guided Multi-layer RECOS Transform

C.-C. Jay Kuo *Fellow, IEEE*

## SCOPE

There is a resurging interest in developing a neural-network-based solution to the supervised machine learning problem. The convolutional neural network (CNN), which is also known as the feedforward neural network and the multi-layer perceptron (MLP), will be studied in this note. To begin with, we introduce a RECOS transform as a basic building block of CNNs. The “RECOS” is an acronym for “REctified-CORrelations on a Sphere” [1]. It consists of two main concepts: 1) data clustering on a sphere and 2) rectification. Afterwards, we interpret a CNN as a network that implements the guided multi-layer RECOS transform with three highlights. First, we compare the traditional single-layer and modern multi-layer signal analysis approaches, point out key ingredients that enable the multi-layer approach, and provide a full explanation to the operating principle of CNNs. Second, we discuss how guidance is provided by labels through backpropagation in the training. Third, we show that a trained network can be greatly simplified in the testing stage demanding only one-bit representation for both filter weights and inputs.

## RELEVANCE

CNNs are widely used in the computer vision field nowadays. They offers state-of-the-art solutions to many challenging vision and image processing problems such as object detection, scene classification, room layout estimation, semantic segmentation, image super-resolution, image restoration, object tracking, etc. They are the main stream machine learning tool for big visual data analytics. A great amount of effort has been devoted to the interpretability of CNNs based on various disciplines and tools, such as approximation theory, optimization theory and visualization techniques. We explain the CNN operating principle using data clustering, rectification, signal transform, which are familiar to researchers and engineers in the signal processing and pattern recognition community. As compared with other studies, this approach appears to be more direct and insightful. It is expected to contribute to further research advancement on CNNs.

## PREREQUISITES

The prerequisites consist of basic calculus, probability and linear algebra. Statistics and approximation techniques could also be useful but not necessary.

## PROBLEM STATEMENT

We will study the following four problems in this note.

- 1) *CNN Architecture Evolution*. The CNN architecture evolution is divided into three generations with a historical perspective.
- 2) *Signal Analysis via Multi-Layer RECOS Transform*. We point out the differences between the single- and multi-layer signal analysis approaches and explain the working principle of the multi-layer RECOS transform.
- 3) *Network Initialization and Guided Anchor Vector Update*. The CNN initialization is viewed as an unsupervised clustering process. Supervised clustering is then achieved by backpropagation using data labels in the training stage.
- 4) *Network Simplification*. One can simplify a network greatly with the 1-bit representation of the input signal and the filter weights. Its theoretical foundation is offered.

## SOLUTION

### A. CNN Architecture Evolution

**Computational Neuron.** A computational neuron (or simply neuron) is the basic operational unit in neural networks. It was first proposed by McCulloch and Pitts in [2] to model the “all-or-none” character of nervous activities. It conducts two operations in cascade: an affine transform of input vector  $\mathbf{x}$  followed by a nonlinear activation function. Mathematically, we can express it as

$$y = f(b), \quad b = T_{\mathbf{a}}(\mathbf{x}) = \sum_{i=1}^N a_i x_i + a_0 \mu = \mathbf{a}^T \mathbf{x} + a_0 \mu = \mathbf{a}'^T \mathbf{x}', \quad (1)$$

where  $y$ ,  $\mathbf{x} = (x_1, \dots, x_N)^T \in R^N$  and  $\mathbf{a} = (a_1, \dots, a_N)^T \in R^N$  are the scalar output, the  $N$ -dimensional input and model parameter vectors, respectively,  $a_0 \mu$  is the bias term,  $f(\cdot)$  denotes a nonlinear activation function, and  $b$  is the intermediate result between the two operations. Furthermore, vectors  $\mathbf{x}' = (\mu, x_1, \dots, x_N)^T \in R^{N+1}$  and  $\mathbf{a}' = (a_0, a_1, \dots, a_N)^T \in R^{N+1}$  are augmented vectors for  $\mathbf{x}$  and  $\mathbf{a}$ , respectively.

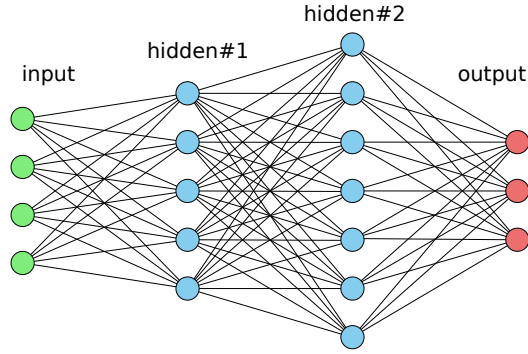


Fig. 1: An exemplary 2G CNN with one input layer, two hidden layers and one output layer.

It is argued in [1] that, if we choose  $\mu = \frac{1}{N} \sum_{i=1}^N x_i$  (i.e. the mean of all input elements)  $a_0$  is a dependent variable in form of  $a_0 = -\sum_{n=1}^N a_n$ . This claim holds by setting  $b = 0$  if  $x_i = c$ ,  $i = 1, \dots, N$ , in Eq. (1), where  $c$  is a non-zero constant. For the vision problem, the input denotes an input image (or image patch). It means that the neuron will not generate a response for a flat input since it does not carry any visual pattern information.

**1G CNN.** The function  $f(\cdot)$  was chosen to be a delayed step function in form of  $f(b) = u(b - \phi)$ , where  $f(b) = 1$  if  $b \geq \phi$  and 0 if  $b < \phi$  in [2]. A neuron is on (in the one-state) if the stimulus,  $b$ , is larger than threshold  $\phi$ . Otherwise, it is off (in the zero-state). Multiple neurons can be flexibly connected into logic networks as models in theoretical neurophysiology. For convenience, we call them the first generation CNNs (1G NNs).

**2G CNN.** Several structured networks were proposed and investigated in 80s and 90s as decision networks for pattern recognition applications. We call them the second generation CNNs (2G CNNs). There are two major advancements from the 1G to 2G NNs. First, 2G NNs have a modularized structure that is suitable for parallel processing. Second, there was no training mechanism in 1G NNs since they were not designed for the machine learning purpose. The backpropagation (BP) technique was introduced in 2G NNs as a training mechanism for supervised learning. Since differentiation is needed in the BP and the step function is not differentiable, new nonlinear activation functions such as the sigmoid function, the rectified linear unit (ReLU) and the parameterized ReLU (PReLU) are introduced.

An exemplary 2G CNN is shown in Fig. 1. It consists of one input, two hidden and one output layers. Each layer consists of a number of nodes. We can label them as layers #1, #2, #3 and #4 in order and denote their node numbers as  $N_1, N_2, N_3$  and  $N_4$ . We have  $N_i$  neurons between the  $(i - 1)$ th and  $i$ th layers ( $i = 2, 3, 4$ ), where each neuron uses all nodes in the  $(i - 1)$ th layer as the input and each node in the  $i$ th layer as the output, called the fully connected layer. 2G CNNs are usually trained as classification networks, where input and output nodes represent selected features and classification types, respectively.

As compared with traditional pattern recognition techniques based on simple linear analysis (e.g. linear discriminant analysis, principal component analysis, etc.), the 2G CNN provides a more flexible mapping from the feature space to the decision space, where the distribution of feature points of one class can be non-convex and irregular. It is built upon a solid theoretical foundation proved by Hornik *et al.* [3] and Cybenko [4]. That is, a CNN with only one hidden layer can be a universal approximator if there are “enough” neurons and “enough” unconfusing training samples. On the other hand, as compared with powerful classifiers such as the support vector machine (SVM) and the random forest (RF) classifiers, the shortcoming of 2G CNNs is their slow convergence rate. The system needs much more training samples to achieve the same classification accuracy.

**3G CNN.** The main difference between 2G and 3G CNNs lies in their input space - the former are features while the latter are source data such as image, video, speech, etc. This is not a trivial generalization. Let us use the LeNet-5 shown in Fig. 2 as an example, whose input is an image of size 32 by 32. Each pixel is an input node. It would be very challenging for the 2G CNN to handle this input since the dimension of the input vector is  $32 \times 32 = 1,024$ . The diversity of possible visual patterns is huge. As explained later, the nodes in the first hidden layer should provide a good representation for the input signal. Thus, it implies a large number of nodes in hidden layers. The number of links (or filter weights) between the input and the first hidden layers is  $N_1 \times N_2$  due to full connection. This number can easily go to the order of millions. If the image dimension is in the order of millions such as those captured by the smart phones nowadays, the solution is clearly unrealistic.

Instead of considering interactions of all pixels in one step as done in the 2G CNN, the 3G CNN decomposes an input image into smaller patches, known as receptive fields for nodes at certain layers. It gradually enlarges the receptive field until the whole image is covered. For example, the filter size of the first two convolutional layers of LeNet-5 is  $5 \times 5$ . The first convolutional layer considers interactions of pixels in the short range. Since the patch size is small, the diversity is less and one can use 6 filters to provide a good approximation to the  $5 \times 5$  source patches. After subsampling, the second convolutional layer examines interaction of pixels in the mid-range. After another subsampling, the whole spatial domain is shrunked to a size  $5 \times 5$  so that it can take global interaction into account using full connection. Typically, the interaction contains not only spatial but also spectral elements (e.g. the RGB three channels and multiple filter responses at the same spatial location) and

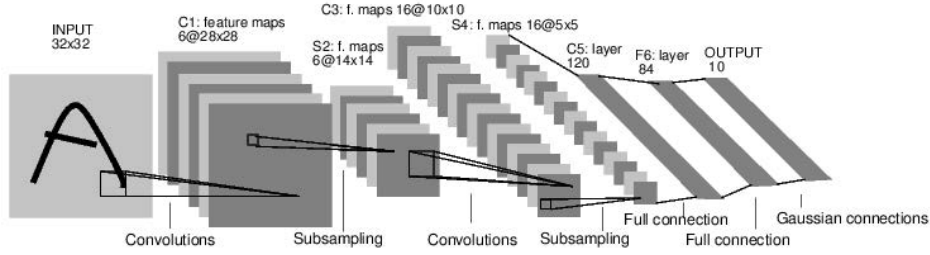


Fig. 2: The LeNet-5 architecture [5] as an exemplary 3G CNN.

all interactions are modeled by computational neurons as given in Eq. (1).

It is typical to decompose a 3G CNN into two subnets: the feature extraction (FE) subnet and the decision making (DM) subnet. The FE subnet consists of multiple convolutional layers while the DM subnet is composed by a couple of fully connected layers. Roughly speaking, the FE subnet conducts clustering aiming at a new representation through a sequence of RECOS transforms. The DM subnet links data representations to decision labels, which is similar to the classification role of 2G CNNs. The exact boundary between the FE subnet and the DM subnet is actually blurred in the LeNet-5. It can be either S4 or C5. If we view S4 as the boundary, then C5 and F6 are two hidden layers of the DM subnet. On the other hand, if we choose C5 as the boundary, then there is only one hidden layer (*i.e.*, F6) in the DM subnet. Actually, since these two subnets are connected side-by-side, the transition from the representation to the classification happens gradually and smoothly.

One main advantage of the 3G CNN over state-of-the-art SVM and RF classifiers is that the feature extraction is automatically done through the BP from the last layer to the first layer. Good features are difficult to find for all classifiers including 2G CNN, SVM and RF. It demands rich domain knowledge, yet there is no guarantee the found features are truly optimal. This explains why the traditional computer vision field is fragmented by different applications. After the emergence of 3G CNNs, the domain knowledge is no more important in feature determination, yet it plays a critical role in labeled datasets construction. To give an example, anaconda, vipers, titanoboa, cobras, rattlesnake, etc. are finer classifications of snakes. It demands expert knowledge to collect and label their images. The CNN provides a powerful tool in data-driven supervised learning. The emphasis is shifted from “extracting features from the source data” to “constructing datasets by pairing carefully selected data and their labels”.

### B. Single-Layer RECOS Transform

Our discussion applies to  $\mathbf{x}$  and  $\mathbf{a}$  if  $\mu = 0$  or augmented vectors  $\mathbf{x}'$  and  $\mathbf{a}'$  if  $\mu \neq 0$ . For convenience, we only consider the case with  $\mu = 0$ . The generalization to the augmented case is straightforward.

**Clustering on Sphere’s Surface.** There is a modern interpretation to the neuron model in Eq. (1) [1]. Let

$$S_X = \left\{ \mathbf{x} \mid \|\mathbf{x}\| = 1 \right\}.$$

be an  $N$ -dimensional unit hyper-sphere (or simply sphere), where we use  $X$  to denote the input set. We consider the clustering problem for points in  $S$  using the geodesic distance. For  $\mathbf{x}$  be a member in  $S$ , we have to normalize it to be with unit length, which does have a physical meaning. If the original magnitude of  $\mathbf{x}$  is  $c$ , it is rescaled by  $\frac{1}{c}$  by normalization. This is equivalent to contrast adjustment if  $\mathbf{x}$  is an image patch. When  $c$  is small, the patch is nearly flat and dark. It carries little information while normalization may amplify noise. In this case, we can simply take it as zero without normalization. For other cases, normalization helps matching and clustering of visual patterns. Clearly, the normalized vector is a point in  $S_X$ .

The geodesic distance of two points,  $\mathbf{x}_i$  and  $\mathbf{x}_j$  in  $S_X$ , is proportional to the magnitude of their angle, which can be computed by

$$\theta(\mathbf{x}_i, \mathbf{x}_j) = \cos^{-1}(\mathbf{x}_i^T \mathbf{x}_j).$$

Since  $\cos \theta$  is a monotonically decreasing function for  $0^\circ \leq |\theta| \leq 180^\circ$ , we can use the correlation  $0 \leq \mathbf{x}_i \mathbf{x}_j^T = \cos \theta \leq 1$  as a distance measure between two vectors, and cluster vectors in  $S$  accordingly. Note that, when  $90^\circ \leq |\theta| \leq 180^\circ$ , the correlation,  $\mathbf{x}_i^T \mathbf{x}_j = \cos \theta$ , is a negative value.

Although one can connect individual neurons to form neural networks via branching and/or merging as done in 1G CNNs, such networks are not useful in machine learning. For 2G and 3G CNNs, a set of neurons are designed to operate on a set of input nodes. For example, nodes in each hidden layer and the output layer in Fig. 1 take the weighted sum of values of nodes in the preceding layer as their outputs. These outputs are treated as one inseparable unit which becomes the input to the next layer. In the signal processing terminology, the set neurons (of filters) form one filter bank. The “Rectified-CORrelations on a Sphere” (RECOS) model [1] describes the relationship between nodes of the  $(l - 1)$ th and  $l$ th layers,  $l = 1, 2, \dots$ , where the input layer is the 0th layer. There are three RECOS units in cascade for the 2G CNN in Fig. 1. One corresponds to a filter bank. The filter weight vector is called an anchor vector since it serves as a reference for a neuron.

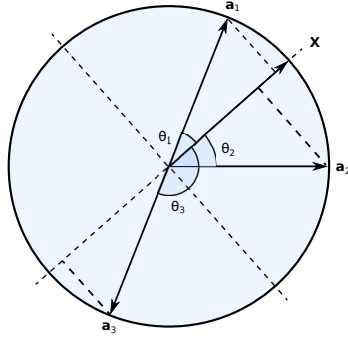


Fig. 3: Illustrate the need of rectification [1].

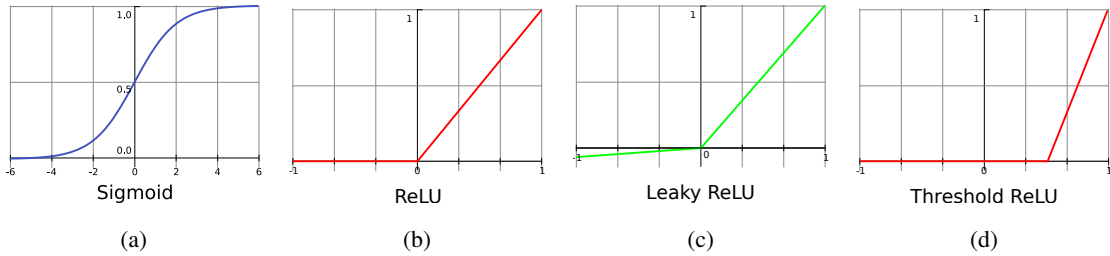


Fig. 4: Illustration of four rectifiers: (a) the sigmoid function, (b) the ReLU (middle), (c) the Leaky ReLU and (d) the Threshold ReLU.

**Need of Rectification.** A neuron computes the correlation between an input vector and its anchor vector to measure their similarity. There are  $K$  neurons in one RECOS unit. Each neuron has a filter weight vector denoted by  $\mathbf{a}_k$ ,  $k = 1, \dots, K$ . The projection of  $\mathbf{x}$  onto anchor vectors  $\mathbf{a}_k$ , can be written in form of

$$\mathbf{y} = \mathbf{A}\mathbf{x}, \quad \mathbf{A}^T = [\mathbf{a}_1 \cdots \mathbf{a}_k \cdots \mathbf{a}_K],$$

where  $\mathbf{y} = (y_1, \dots, y_k, \dots, y_K)^T \in R^K$ ,  $y_k = \mathbf{a}_k^T \mathbf{x}$  and  $\mathbf{A} \in R^{K \times N}$ . For input vectors  $\mathbf{x}_i$  and  $\mathbf{x}_j$ , their corresponding outputs are  $y_i$  and  $y_j$ . If the geodesic distance of  $\mathbf{x}_i$  and  $\mathbf{x}_j$  in  $S_X$  is close, we expect that the geodesic distance of  $y_i$  and  $y_j$  in the  $K$ -dimensional unit sphere,  $S_Y$ , to be close as well.

To show the necessity of rectification, a 2D example is illustrated in Fig. 3, where  $\mathbf{x}$  and  $\mathbf{a}_k$  ( $k = 1, 2, 3$ ) denote an input and three anchor vectors on the unit circle, respectively, and  $\theta_i$  is their respective angle. Since  $\theta_1$  and  $\theta_2$  are less than 90 degrees,  $\mathbf{a}_1^T \mathbf{x}$  and  $\mathbf{a}_2^T \mathbf{x}$  are positive. The angle,  $\theta_3$ , is larger than 90 degrees and correlation  $\mathbf{a}_3^T \mathbf{x}$  is negative. The two vectors,  $\mathbf{x}$  and  $\mathbf{a}_3$ , are far apart in terms of the geodesic distance. Since  $\cos \theta$  is monotonically decreasing for  $0^\circ \leq |\theta| \leq 180^\circ$ , it is fine to use it to reflect the geodesic distance in one layer.

However, when two RECOS units are in cascade, the filter weights of the 2nd RECOS unit can take either positive or negative values. If the response of the 1st RECOS unit is negative, the product of a negative response and a negative filter weight will produce a positive value. Yet, the product of a positive response and a positive filter weight will also produce a positive value. As a result, the system cannot differentiate these two cases. The geodesic distance of  $\mathbf{x}$  and  $-\mathbf{x}$  should be farthest. However, they yield the same result under the above-mentioned scenario. Similarly, a system without rectification cannot differentiate the following two cases: 1) a positive response at the first layer followed by a negative filter weight at the second layer; and 2) a negative response at the first layer followed by a positive filter weight at the second layer.

**Rectifier Design.** Since a nonlinear activation unit is used to rectify correlations, it is called a rectifier. To avoid confusion of the above-mentioned cases, we impose the following two requirements on a rectifier.

- 1) The output  $\mathbf{a}_k^T \mathbf{x}$  should be rectified to be a nonnegative value.
- 2) The rectification function should be monotonically increasing so as to preserve the order of the geodesic distance.

Three rectifiers are often used by CNNs in recent years. They are the sigmoid function, the rectified linear unit (ReLU) and the parameterized ReLU (PReLU) as shown in Figs. 4(a)-(c). The PReLU is also known as the leaky ReLU. Both the sigmoid and ReLU satisfy the above two requirements. Although the PReLU does not satisfy the first requirement strictly, it does not have a severe negative impact on spherical surface clustering. This is because a negative correlation is rectified to a significantly smaller value.

Based on the two requirements, one can design different rectifiers to serve the same objective. One example is shown in Fig. 4(d). It is called the threshold ReLU (TReLU). The rectification function can be defined as  $\text{TReLU}(x) = 0$ , if  $x < \phi$  and  $\text{TReLU}(x) = \frac{x-\phi}{1-\phi}$  if  $x \geq \phi$ . When  $\phi = 0$ , TReLU is reduced to ReLU. For the LeNet-5 applied to the MNIST dataset, we

observe better performance as  $\phi$  increases from 0 to 0.5 and then decreases. One advantage of  $\text{TReLU}(\phi)$  with  $\phi > 0$  is that we can block the influence of more anchor vectors. When  $\phi = 0$ , we block the influence of anchor vectors that have an angle larger than 90 degrees with respect to the input vector. When  $\phi = 0.5$ , we block the influence of anchor vectors that have an angle larger than 60 degrees. Apparently, the latter leads to a sparser system than the former.

### C. Multi-layer RECOS Transform

**Single-Layer Signal Analysis via Representation.** Signal modeling and representation is commonly used in the signal processing field for signal analysis. Typically, we have a linear model in form of

$$\mathbf{x} = \mathbf{A}\mathbf{c}, \quad (2)$$

where  $\mathbf{x} \in R^N$  denotes the signal of interest,  $\mathbf{A} \in R^{N \times M}$  is a representation matrix and  $\mathbf{c} \in R^M$  is the coefficient vector. If  $M = N$  and the column vectors of  $\mathbf{A}$  form a set of basis functions, Eq. (2) defines a transform from one basis to another. The task is in selecting powerful basis functions to represent signals of interest. Fourier and wavelet transforms are famous examples. A subset of coefficient vector  $\mathbf{c}$  can be used as the feature vector. If  $M > N$ , there exist infinitely many solutions in  $\mathbf{c}$ . We can impose some constraints on  $\mathbf{c}$ , leading to the linear least-squares solution, sparse coding, among others. For the sparse representation, the task is in finding a good dictionary,  $\mathbf{A}$ , to represent the underlying signal. Again, a subset of coefficient vector  $\mathbf{c}$  can be chosen as features.

**Multi-Layer Signal Analysis via Cascaded Transforms.** The CNN approach provides a brand new framework for signal analysis. Instead of finding a representation for signal analysis, it relies on a sequence of cascaded transforms that builds a link between the input signal and the output decision. The operation in a transform is to conduct spherical surface's clustering of input samples with a rectified output (i.e. the RECOS transform).

For 2G CNNs, each network corresponds to a simple cascade of multiple RECOS transforms in a row. Mathematically, we have

$$\mathbf{d} = \mathbf{B}_L \cdots \mathbf{B}_l \cdots \mathbf{B}_1 \mathbf{x}, \quad (3)$$

where  $\mathbf{x}$  is the input signal,  $\mathbf{d} = (d_1, \cdots, d_c, \cdots, d_C)$  is the output vector in the decision space indicating the likelihood in class  $c$  with  $c = 1, \cdots, C$ , and  $\mathbf{B}_l$  is the  $l$ -layer RECOS transform matrix with  $l = 1, \cdots, L$ . The input and output to the  $l$ -layer RECOS transform  $\mathbf{B}_l$  are denoted by  $\mathbf{x}_l$  and  $\mathbf{x}_{l-1}$ . Thus, we get

$$\mathbf{x}_l = \mathbf{B}_l \mathbf{x}_{l-1}, \quad \mathbf{B}_l = \mathbf{R} \circ \mathbf{A}_l, \quad (4)$$

where  $\mathbf{R}$  is the element-wise rectification function operating on the output of  $\mathbf{A}_l \mathbf{x}_l$ . Clearly, we have  $\mathbf{x}_0 = \mathbf{x}$  and  $\mathbf{x}_L = \mathbf{d}$ .

The ground truth is that  $d_i = 1$  if  $i$  is the target class while  $d_j = 0$  if  $j$  is not the target class, which is called the one-hot vector. The training samples have both input  $\mathbf{x}$  and its label in form of  $\mathbf{d}$ . The testing samples have only the input and we need to predict its output  $\mathbf{d}$  and convert it to its nearest one-hot vector. The task is in finding good  $\mathbf{B}_l$ ,  $l = 1, \cdots, L$ , so as to minimize the classification error.

For 3G CNNs, we have two types of  $\mathbf{B}_l$  in form of:

$$\mathbf{B}_l^C = \mathbf{P} \bigcup_{s \in \Omega} \mathbf{R} \circ \mathbf{A}_{l,s}, \quad \text{and} \quad \mathbf{B}_l^F = \mathbf{R} \circ \mathbf{A}_l, \quad (5)$$

where  $\mathbf{A}_{l,s}$  denotes a convolutional filter at layer  $l$  with spatial index  $s$ ,  $\bigcup_s$  is the union of outputs from a neighborhood,  $\Omega$ , and  $\mathbf{P}$  denotes a pooling operation. The union of outputs from a set of parallel convolutional filters serve as the input to the filter at the next layer. The two RECOS transforms,  $\mathbf{B}_l^C$  and  $\mathbf{B}_l^F$ , are called the convolutional layer and the fully connected layer, respectively, in the modern CNN literature. Clearly,  $\mathbf{B}_l = \mathbf{B}_l^F$  in Eq. (4).

It is inspiring to compare the two signal analysis approaches as given in Eqs. (2) and (3). The one in Eq. (2) is the single layer approach where no rectification is needed. The one in Eq. (4) is the multi-layer approach and rectification is essential. The single layer approach seeks for a better signal representation scheme. For example, a multiple-scale signal representation was developed using the wavelet transform. A sparse signal representation scheme was proposed using a trained dictionary. The objective is to find an "optimal" representation to separate critical components in signals from others.

In contrast, the CNN approach does not intend to decompose underlying signals. Instead, it adopts a sequence of RECOS transforms to cluster input data based on their similarity layer by layer until the output layer is reached. The output layer predicts the likelihood of all possible decisions (e.g., object classes). The training samples provide a relationship between an image and its decision label. The CNN can predict results even without any supervision, although the prediction accuracy would be low. The training samples guide the CNN to form more suitable anchor vectors (thus better clusters) and connect clustered data with decision labels. To summarize, we can express the multi-layer RECOS transform as

$$\begin{aligned} \text{2G CNN:} \quad & \mathbf{x} = \mathbf{x}_0 \xrightarrow{\mathbf{B}_1^F} \mathbf{x}_1 \xrightarrow{\mathbf{B}_2^F} \cdots \xrightarrow{\mathbf{B}_{L-1}^F} \mathbf{x}_{L-1} \xrightarrow{\mathbf{B}_L^F} \mathbf{x}_L = \mathbf{d}, \\ \text{3G CNN:} \quad & \mathbf{x} = \mathbf{x}_0 \xrightarrow{\mathbf{B}_1^C} \mathbf{x}_1 \xrightarrow{\mathbf{B}_2^C} \cdots \xrightarrow{\mathbf{B}_m^C} \mathbf{x}_m \xrightarrow{\mathbf{B}_{m+1}^F} \mathbf{x}_{m+1} \xrightarrow{\mathbf{B}_{m+2}^F} \cdots \xrightarrow{\mathbf{B}_{L-1}^F} \mathbf{x}_{L-1} \xrightarrow{\mathbf{B}_L^F} \mathbf{x}_L = \mathbf{d}, \end{aligned}$$

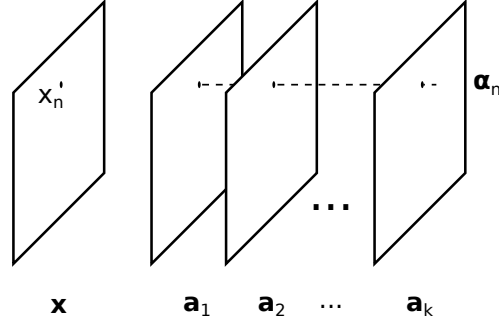


Fig. 5: Visualization of anchor-position vector  $\alpha_n$  [1].

The output from the  $l$ th layer,  $\mathbf{x}_l$ , serves as the input to the  $(l + 1)$ th layer. It is called the intermediate representation at the  $l$ th layer or the  $l$ th intermediate representation in short.

It is important to have a deeper understanding on the compound effect of two cascaded RECOs transforms. Here, we state the main result in [1]. A representative 2D input and its corresponding anchor vectors are shown in Fig. 5.  $\alpha_n$  is a  $K$ -dimensional vector formed by the same position (or element) of  $\mathbf{a}_k$ . It is called the anchor-position vector since it captures the position information of anchor vectors. Although anchor vectors  $\mathbf{a}_k$  capture global representative patterns of  $\mathbf{x}$ , they are weak in capturing position sensitive information. This shortcoming can be compensated by modulating outputs with elements of anchor-position vector  $\alpha_n$  in the next layer.

Let us use layers S4, C5 and F6 in LeNet-5 as an example. There are 120 anchor vectors of dimension 400 from S4 to C5. We collect 400 anchor-position vectors of dimension 120, multiply the output at C5 by them to form a set of modulated outputs, and then compute 84 anchor vectors of dimension 120 from C5 to F6. Note that the output at C5 contains primarily the spectral information but not the position information. If a position in the input vectors has less consistent information, the variance of its associated anchor position vector will be larger and the modulated output will be more random. As a result, its impact on the formation of the 84 anchor vectors is reduced. For more details, we refer to the discussion in [1].

**New Clustering Representation.** We have a one-to-one association between a data sample and its cluster in traditional clustering schemes. However, this is not the case in the RECOs transform. A new clustering representation is adopted by the CNN. That is, for an input vector  $\mathbf{x}$ , the RECOs transform generates a set of  $K$  non-negative correlation values as the output vector of dimension  $K$ . This representation enables repetitive clustering layer by layer as given in Eq. (4). For an input, one can determine the significance of clusters according to the magnitude of the rectified output value. If its magnitude for a cluster is zero,  $\mathbf{x}$  is not associated with that cluster. A cluster is called a relevant or irrelevant one depending on whether it has an association with  $\mathbf{x}$ . Among all relevant ones, we call cluster  $i$  the “primary” cluster for input  $\mathbf{x}$  if

$$i = \arg \max_k \mathbf{a}_k^T \mathbf{x}.$$

The remaining relevant ones are the “auxiliary” clusters.

The FE subnet uses anchor vectors to capture local, mid-range and long-range spatial patterns. It is difficult to predict the clustering structure since new information is introduced at a new layer. The DM subnet attempts to reduce the dimension of intermediate representations until it reaches the dimension of the decision space. We observe that the clustering structure becomes more obvious as the layer of the DM subnet goes deeper. That is, the output value of the primary is closer to unity while the number of auxiliary clusters is fewer and their output values are closer to zero. Under this scenario, an anchor vector provides a good approximation to the centroid for the corresponding cluster.

The choice of anchor vector numbers,  $K_l$ , at the  $l$ th layer is an important problem in the network design. If input data  $\mathbf{x}_{l-1}$  has a clear clustering structure (say, with  $h$  clusters), we can set  $K_l = h$ . However, this is often not the case. If  $K_l$  is set to a value too small, we are not able capture the clustering structure of  $\mathbf{x}_{l-1}$  well, and it will demand more layers to split them. If  $K_l$  is set to a value too large, there are more anchor vectors than needed and a stronger overlap between rectified output vectors will be observed. As a result, we still need more layers to separate them. Another way to control the clustering process is the choice of the threshold value,  $\phi$ , of the TReLU. A higher threshold value can reduce the negative impact of a larger  $K_l$  value. The tradeoff between  $\phi$  and  $K_l$  is an interesting future research topic.

#### D. Network Initialization and Guided Anchor Vector Update

Data clustering techniques play a critical role in the understanding of the underlying structure of data. The k-means algorithm, which is probably the most well-known clustering method, has been widely used in pattern recognition and supervised/unsupervised learning. As discussed in the last subsection, each CNN layer conducts data clustering on the surface

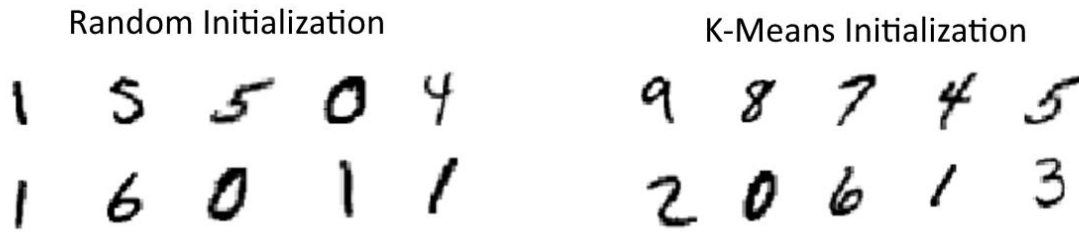


Fig. 6: Comparison of MNIST unsupervised classification results of the LeNet-5 architecture with the random (left) and k-means (right) and initializations, where the images that are closest to centroids of ten output nodes are shown.

of a high-dimensional sphere based on a rectified geodesic distance. Here, we would like to understand the effect of multiple layers in cascade from the input data source to the output decision label. For unsupervised learning such as image segmentation, several challenges exist in data clustering [6]. Questions such as “what is a cluster?” “how many clusters are present in the data?” “are the discovered clusters and partition valid?” remain open. These questions reveal the fundamental limit of unsupervised data clustering methods.

In the context of supervised learning, traditional feature-based methods extract features from data, conduct clustering in the feature space and, finally, build a connection between clusters and decision labels. Although it is relatively easy to build a connection between the data and data labels through features, it is challenging to find effective features. In this setting, the dimension of the feature space is usually significantly smaller than that of the data space. As a consequence, it is unavoidable to sacrifice rich diversity of input data. Furthermore, the feature selection process is guided by humans based on their domain knowledge (i.e. the most discriminant properties of different objects). This process is nevertheless heuristic. It can get overfit easily. Human efforts are needed not only in data labeling but also in feature design.

The CNN is a supervised learning system, where supervision is conducted by a training process using labeled data. This supervision closes the gap between low-level representations (*e.g.*, the pixel representation) and high-level semantics, which is known as the semantic gap. Although there has been active research on weakly-supervised CNNs, we will focus on fully supervised CNNs in the discussion below since it is a more mature topic. A CNN offers a powerful solution to address above-mentioned difficulties for supervised learning.

**Network Initialization.** In contrast with the traditional feature-based classification approach, human efforts are only demanded in data labeling. The CNN conducts a sequence of representation transforms using cascaded RECO units. The dimension of transformed representations gradually decreases until it reaches the number of output classes. Since labels of output classes are provided by humans with a semantic meaning, the whole end-to-end process is called the *guided* (or supervised) transform.

Before examining the effect of label guidance, we first compare two network initialization schemes: 1) the random and 2) the k-means initializations. For the latter, we perform k-means at each layer based on its corresponding input data samples, and repeat this process from the input to the output layer after layer. Random initialization is commonly adopted in practice nowadays. Although the k-means initialization was discussed in the literature, no convincing evidence has so far been offered to show its superiority over the random initialization. Based on the above discussion, we expect the k-means initialization to be a better choice. This is verified by our experiments in the LeNet-5 applied to the MNIST dataset as given below. The generalization to more complicated networks and datasets is under way.

Once the network is initialized, we can pass the test data through the network and observe the output, which corresponds to unsupervised learning. The comparison of unsupervised classification results with the random and k-means initializations in Fig. 6, where we show images that are closest to the anchor vectors of the ten output nodes. We see that the k-means initialization provides ten anchor vectors pointing to ten different digits while the random initialization cannot do the same. Different random initializations will lead to different results, yet the one given in Fig. 6 is representative. That is, multiple anchor vectors point to the same digit.

**Guided Anchor Vector Update.** We apply the BP to train the network with a varying number of training samples. For a fixed number of training samples, we train the network until its performance converges and plot the correct classification rate in Fig. 7. The two points along the y-axis indicate the correct classification rates without any training sample. The rates are around 32% and 14% for the k-means and random initializations, respectively. Note that the 14% is slightly better than the random guess on the outcome, which is 10%. Then, both curves go up as the number of training samples grows. The k-means can reach about 90% correct classification rate when the number of training samples is around 250, which is only 0.41% of the entire MNIST training dataset (*i.e.* 60K samples). This shows the power of the LeNet-5 even under extremely low supervision.

To further understand the role played by label guidance, we examine the impact of the BP on the orientation of anchor vectors in various layers. We show in Table I the averaged orientation changes of anchor vectors in terms of radian (or degree) for the two cases in Fig. 6. They are obtained after the convergence of the network with all 60,000 MNIST training samples.

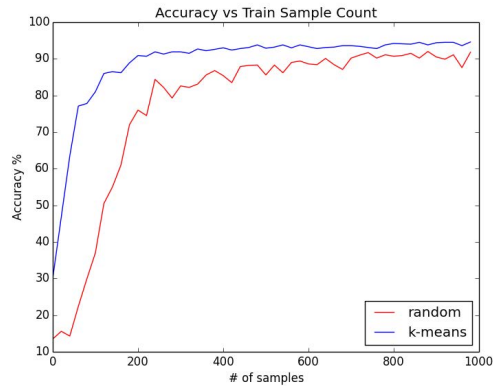


Fig. 7: Comparison of MNIST weakly-supervised classification results of the LeNet-5 architecture with the random and k-means initialization schemes, where the correct classification rate is plotted as a function of training sample numbers.

In/Out layers	k-means	random
Input/S2	0.155 (or 8.881 $^{\circ}$ )	1.715 (or 98.262 $^{\circ}$ )
S2/S4	0.169 (or 9.683 $^{\circ}$ )	1.589 (or 91.043 $^{\circ}$ )
S4/C5	0.204 (or 11.688 $^{\circ}$ )	1.567 (or 89.783 $^{\circ}$ )
C5/F6	0.099 (or 5.672 $^{\circ}$ )	1.579 (or 90.470 $^{\circ}$ )
F6/Output	0.300 (or 17.189 $^{\circ}$ )	1.591 (or 91.158 $^{\circ}$ )

TABLE I: The averaged orientation changes of anchor vectors in terms of the radian (or degree) for the k-means and the random initializations.

This orientation change is the result due to label guidance through the BP. It is clear from the table that, a good network initialization (corresponding to unsupervised learning) leads to a faster convergence rate in supervised learning.

**Classes and Sub-Classes.** We use another example to gain further insights to the guided clustering. That is, we zoom into the horned rattlesnake class obtained by the AlexNet and conduct the unsupervised k-means on feature vectors in the last layer associated with this class to further split it into multiple sub-classes. Images of two sub-classes are shown in Fig. 8. Images in the same sub-classes are visually similar. However, they are not alike across sub-classes. The two sub-classes are grouped together under the horned rattlesnake class just because they share the same class label (despite strong visual dissimilarity). That shows the power of label guidance. However, the feature distance is shorter for images in the same sub-class and longer for images in different sub-classes. This is due to the inherent clustering capability of CNNs.

### E. Network Simplification

The number of bits required to represent filter weights is a practical question in CNN hardware implementation. It has been observed that there is little performance degradation in the correct classification rate when the number of bits is reduced. This can be easily explained using the anchor vector viewpoint.



Fig. 8: Two sub-classes obtained from the horned rattlesnake class using unsupervised clustering.

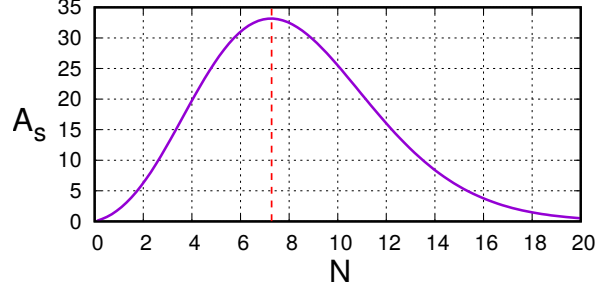


Fig. 9: The plot of the total surface area of the  $N$ -dimensional unit sphere as a function of  $N$ .

Let  $\mathbf{a} = (a_1, \dots, a_N)^T \in R^N$  be the  $N$ -dimensional anchor vector in the  $N$ -dimensional unit sphere. Thus, we have  $-1 \leq a_i \leq 1$ ,  $i = 1, \dots, N$ . Its total dynamic range is 2. By quantizing the interval with  $b$  bits uniformly, we obtain  $2^b$  values for each  $a_i$ . Then, there are  $(2^b)^N = 2^{bN}$  possible combinations. Now, we need to normalize each possible outcome by its magnitude so that they will be on the surface of the  $N$ -dimensional sphere. It offers a projection from the uniform lattice points in a  $N$ -dimensional cube onto the  $N$ -dimensional sphere. On one hand, the projected points are not uniformly distributed on sphere's surface, which can be easily verified using a 2-D example. On the other hand, we can examine the statistic behavior; namely, the ‘‘averaged’’ density of projected points.

The averaged density,  $D$ , of anchor vectors and its inverse can be written as

$$D = \frac{2^{bN}}{A_S(N)}, \quad D^{-1} = A_S(N)2^{-bN},$$

where  $b$  is the number of bits for filter weights,  $N$  is the number of input elements,  $A_S(N)$  is the total surface area of the  $N$ -dimensional unit sphere, and  $D^{-1}$  is the averaged coverage per anchor point. The quantization error caused by the finite-bit representation is proportional to the averaged coverage per anchor vector. Clearly, a smaller coverage will result in a smaller quantization error. The value of  $A_S(N)$  as a function of  $N$  is plotted in Fig. 9. It increases from 1 to 7, reaches the maximum at 7.25695 and then decreases afterwards. It goes to zero asymptotically. Although bit number  $b$  decreases the quantization error in  $O(2^{-b})$ , the input dimension,  $N$ , plays an even more significant role since it decreases the quantization error in  $O(A_S(N)2^{-N})$ .

Consider the case  $b = 1$ . We quantize  $a_i$  based on its sign (i.e. the sign bit) and set it to either 1 or -1. Then, the weighted sum  $\sum_i^N a_i x_i$  can be simplified to addition or subtraction of elements of the input. Note that the normalization factor,  $\frac{1}{\sqrt{N}}$ , can be pulled out and applied afterwards after the summation. The quantization error decreases in  $O(A_S(N)2^{-N})$ . For most CNNs, the  $N$  value is often in the order of hundreds or thousands. The smallest  $N$  in the LeNet-5 is 25 ( $= 5 \times 5$ ) occurring at the first layer. For a color input image with a filter size of  $3 \times 3$ , the smallest  $N$  value is 27 ( $= 3 \times 3 \times 3$ ) which also occurs at the first layer. This justifies the use of the 1-bit resolution in representing filter weights.

The above argument applies not only to the filter weight vector,  $\mathbf{a} = (a_1, \dots, a_N)^T \in R^N$ , but also the input vector,  $\mathbf{x} = (x_1, \dots, x_N)^T \in R^N$ . Thus, we can use 1-bit (i.e. the sign bit) to represent both and get a network that demands only the bit operation. A good classification result for the ImageNet dataset with this greatly simplified network was reported empirically in [7]. Here, a theoretical justification is offered.

#### F. Discussion and Open Issues

Several well known facts can be well explained based on the interpretation given above.

- **Robustness to wrong labels.** Humans do clustering first and then the CNN mimics humans based on the statistics of all labeled samples. It can tolerate small percentages of erroneous labels since these wrongly labeled data do not have a major impact on clustering results.
- **No overfitting.** Overfitting occurs when a statistic model describes noise instead of the underlying input/output relationship. For a given number of observations, this could happen for an excessively complex model that has too many model parameters. Such a model has poor prediction performance since it over reacts to minor fluctuations in the training data. Although a CNN has a large number of parameters (namely, filter weights), it does not suffer from overfitting. This can be explained as follows. When there are only input and output layers without any hidden layers in between, the CNN solves a linear least-squared regression problem (where no rectification is needed.) It is well known the linear regression is robust to noisy data. When there are hidden layers, the filter weight determination is a cascaded optimization problem, which has to be solved iteratively. In the BP process, we update the filter weights layer by layer in a backward direction. Fundamentally, it still attempts to solve a regression problem at each layer. Although a rectifier conducts rectification on the output, it does not change its regression nature.

- **Data augmentation.** A low-cost way to generate more samples is data augmentation. This is feasible since minor perturbations in the image pixel domain do not change their class types typically.
- **Dataset bias.** The CNN can be biased due to the inherent bias existing in training samples. It is well known that the performance of a CNN can degrade significantly from one dataset to the other in the same application domain due to this reason.

Although a CNN can be well explained as a guided multi-layer RECOs transform process, many open problems still remain.

- **Network Architecture Design.** It is interesting to be able to specify the layer number and the filter number per layer for given applications.
- **Decoder Network Analysis.** The classification network maps an image to a label. There are image processing networks that accept an image as the input and another image as the output. Examples include super-resolution networks, semantic segmentation networks, etc. These networks can be decomposed into an encoder-decoder architecture. The analysis in this note focuses on the encoder part. It is interesting to generalize the analysis to the decoder part as well.
- **Localization and Attention.** Region proposals have been used in object detection to handle the object localization problem. It is desired to learn the object location and human visual attention from the network automatically without the use of proposals. The design and analysis of networks to achieve this goal is interesting.
- **Transfer Learning.** It is often possible to finetune a CNN for a new application based on an existing CNN model trained by another dataset in another application. This is because the low-level image representation corresponding to the beginning CNN layers can be very flexible and equally powerful.
- **Weakly Supervised Learning.** Unsupervised and Heavily supervised learning are two extremes. Weakly supervised learning occurs most frequently in our daily applications. The design and analysis of weakly supervised networks is important and practical.

## CONCLUSION

The operating principle of CNNs was clearly explained as a guided multi-layer RECOs transform system in this note. A couple of illustrative examples were provided to support the discussion. Several well known facts were explained based on our interpretation and some open issues were pointed out.

## ACKNOWLEDGEMENT

The author would like to thank the help from Andrew Szot, Shangwen Li, Zhehang Ding and Gloria Budiman in running experiments and drawing figures for this work. This material is based on research sponsored by DARPA and Air Force Research Laboratory (AFRL) under agreement number FA8750-16-2-0173. The U.S. Government is authorized to reproduce and distribute reprints for Governmental purposes notwithstanding any copyright notation thereon. The views and conclusions contained herein are those of the authors and should not be interpreted as necessarily representing the official policies or endorsements, either expressed or implied, of DARPA and Air Force Research Laboratory (AFRL) or the U.S. Government.

## AUTHOR

C.-C. Jay Kuo (cckuo@ee.usc.edu) is a Professor of Electrical Engineering at the University of Southern California, Los Angeles, California, USA.

## REFERENCES

- [1] C.-C. J. Kuo, "Understanding convolutional neural networks with a mathematical model," *Journal of Visual Communication and Image Representation*, vol. 41, pp. 406–413, 2016.
- [2] W. S. McCulloch and W. Pitts, "A logical calculus of the ideas immanent in nervous activity," *The Bulletin of Mathematical Biophysics*, vol. 5, no. 4, pp. 115–133, 1943.
- [3] K. Hornik, M. Stinchcombe, and H. White, "Multilayer feedforward networks are universal approximators," *Neural networks*, vol. 2, no. 5, pp. 359–366, 1989.
- [4] G. Cybenko, "Approximation by superpositions of a sigmoidal function," *Mathematics of control, signals and systems*, vol. 2, no. 4, pp. 303–314, 1989.
- [5] Y. LeCun, L. Bottou, Y. Bengio, and P. Haffner, "Gradient-based learning applied to document recognition," *Proc. IEEE*, vol. 86, no. 11, pp. 2278–2324, 1998.
- [6] A. K. Jain, "Data clustering: 50 years beyond k-means," *Pattern recognition letters*, vol. 31, no. 8, pp. 651–666, 2010.
- [7] M. Rastegari, V. Ordonez, J. Redmon, and A. Farhadi, "Xnor-net: Imagenet classification using binary convolutional neural networks," in *European Conference on Computer Vision*. Springer, 2016, pp. 525–542.